J Eng Math (2006) 56:415–435
DOI 10.1007/s10665-006-9051-4

ORIGINAL PAPER

An anisotropic model of the Mullins effect

M. H. B. M. Shariff

Received: 9 December 2004 / Accepted: 3 April 2006 /
Published online: 21 September 2006

Abstract The Mullins effect in rubber-like materials is inherently anisotropic. However, most constitutive models developed in the past are isotropic. These models cannot describe the anisotropic stress-softening effect, often called the Mullins effect. In this paper a phenomenological three-dimensional anisotropic model for the Mullins effect in incompressible rubber-like materials is developed. The terms, damage function and damage point, are introduced to facilitate the analysis of anisotropic stress softening in rubber-like materials. A material parametric energy function which depends on the right stretch tensor and written explicitly in terms of principal stretches and directions is postulated. The material parameters in the energy function are symmetric second-order damage and shear-history tensors. A class of energy functions and a specific form for the constitutive equation are proposed which appear to simplify both the analysis of the three-dimensional model and the calculation of material constants from experimental data. The behaviour of tensional and compressive ground-state Young's moduli in uniaxial deformations is discussed. To further justify our model we show that the proposed model produces a transversely anisotropic non-virgin material in a stress-free state after a simple tension deformation. The proposed anisotropic theory is applied to several types of homogenous deformations and the theoretical results obtained are consistent with expected behaviour and compare well with several experimental data.

Keywords Anisotropic · Constitutive model · Mullins effect · Stress-softening

1 Introduction

When a filled rubber is subjected to cyclic loading it exhibits a stress-softening phenomenon widely known as the Mullins effect [1]. For example, the pressure required to inflate a balloon is noticeably reduced by

M.H.B.M. Shariff (✉)
School of Computing, University of Teesside,
Middlesbrough, UK
Currently at: Etisalat University College,
Sharjah, UAE
e-mail: shariff@ece.ac.ae

prestretching it several times prior to its primary inflation. The Mullins effect has been excellently and comprehensively described by many authors [1–7] and hence we avoid its description here. In the past, the Mullins effect was mainly described by isotropic models. However, there is increasing evidence that the Mullins effect is not, in general, isotropic [1, 8]. This evidence, for example, can be found in a pure shear experiment by Gough [9]; it was found that, after a simple tension deformation from a virgin state, the subsequent pure shear in an orthogonal direction produced a stiffness that is almost as great as for the virgin pure shear deformation. Further anisotropic evidence can also be found, e.g., in an homogeneous plane-strain compression experiment by Pawelski [10]; after loading and unloading the block is rotated by 90 degrees and compressed the material behaved almost like the virgin one which indicates that the softening in the first direction has hardly any influence on the direction orthogonal to the first. In a simple shear experiment of Muhr et al. [11] simple shear loadings in different directions produce different loads.

In this paper, based on the preliminary work of Shariff [12, 13], we develop a model which describes the anisotropic behaviour of the Mullins effect, treated as a quasi-static phenomenon. We concentrate on the Mullins effect and are not concerned with hysteresis, residual strain, thermal and viscoelastic effects. The proposed model is purely phenomenological and does not take into account the underlying physical structure of the material; hence it can be applied to any material exhibiting the Mullins effect.

We assume the virgin material is isotropic with respect to an undeformed and unstressed state. In Sect. 2.2 we define the terms, damage function, which depends on the principal stretches, and damage point, which depends on the principal directions and the history of the right stretch tensor. In Sect. 2.3 we introduce shear-history parameters which also depend on the principal directions and the history of the right stretch tensor. To describe anisotropic stress-softening behaviour, a parametric energy function which depends explicitly on the principal stretches and principal directions is proposed. The parameters in the energy function are the damage tensor, which contains the damage points, and the shear-history tensor which contains the shear-history parameters. Both tensors are second order and symmetric.

In this paper only a class of energy functions which is a subset of a wider class proposed in Sect. 3 is considered. A specific form of this special class is employed and this form seems to simplify the analysis of the three-dimensional model and the calculation for material constants from experimental data discussed in Sect. 6. In Sect. 3.3 energy dissipation is shown via the Clausius–Duhem inequality by treating the damage tensor as an internal variable. In Sect. 4 we show that tensional and compressive directional ground state Young's moduli in uniaxial deformations are in general different. We also reveal that the proposed model produces a transversely anisotropic non-virgin material in a stress-free state after a simple tension deformation as suggested by Horgan et al. [6]. To demonstrate the capabilities of the proposed theory, several anisotropic results are given in Sect. 5 for several types of homogeneous deformations. These results are also compared, qualitatively, with published experimental data. Finally, in Sect. 6, we use our model to fit and predict, quantitatively, simple tension and pure-shear experimental data.

2 The proposed model

2.1 Basic kinematics

We first recall some essential kinematics of finite deformation of an incompressible material. Consider a body occupying the region B_0 in some reference stress-free configuration. Let $\boldsymbol{A}$ be the deformation tensor and $\boldsymbol{X}$ a position vector of a point in B_0. Under this deformation the point moves to a new position $\boldsymbol{x}(\boldsymbol{X}) \in B$, where B is the current configuration of the deformed body.

The current principal stretch λ_i is given by

$$\lambda_i = \sqrt{\boldsymbol{e}_i \bullet \boldsymbol{U}^2 \boldsymbol{e}_i}\,, \tag{1}$$

where $U = \sqrt{\boldsymbol{A}^T\boldsymbol{A}}$ is the right stretch tensor, $\boldsymbol{e}_i$ $(i = 1, 2, 3)$ are the current principal directions of $\boldsymbol{U}$. We write, e.g., λ_i, $\boldsymbol{e}_i$, $\boldsymbol{U}$, etc instead of $\lambda_i(t)$, $\boldsymbol{e}_i(t)$, $\boldsymbol{U}(t)$, etc to denote current variables, where t represents the current time. Due to the incompressibility constraint the principal stretches must satisfy the relation $\lambda_1\lambda_2\lambda_3 = 1$.

2.2 Damage function and damage point

Damage functions are important tools for analysing stress-softening materials. In previous isotropic models [4, 5, 14] softening effects are governed by their "damage" functions and their corresponding damage points (sometimes referred as softening points [5] or maximum-loading parameters [15]). In this section we define a damage function g (which may depend on the material properties) such that $0 = g(1) \leq g(x)\,, \quad x > 0\,, \quad x \in R$ and g increases (strictly) monotonically as x moves away from the point $x = 1$.

It can be easily seen that

$$s_{i,\min} \leq \lambda_i \leq s_{i,\max}, \tag{2}$$

where

$$s_{i,\max} = \max_{0\leq z\leq t} \sqrt{\boldsymbol{e}_i \bullet \boldsymbol{U}^2(z)\boldsymbol{e}_i}\,, \quad s_{i,\min} = \min_{0\leq z\leq t} \sqrt{\boldsymbol{e}_i \bullet \boldsymbol{U}^2(z)\boldsymbol{e}_i}\,, \quad (i = 1, 2, 3); \tag{3}$$

the material is subjected to a deformation history up to the current time t and z denotes a running time variable. Physically, $s_{i,\max}$ and $s_{i,\min}$ are the maximum and minimum strain values, respectively, of the principal-direction line elements throughout the history of the deformation. Note that they are not the maximum and minimum values of the principal stretches throughout the history of the deformation. From the above equation it is clear that $s_{i,\max} \geq 1$ and $s_{i,\min} \leq 1$ and λ_i is bounded by $s_{i,\max}$ and $s_{i,\min}$. However, they are not the only bounds on λ_i. We can construct, for example, the bound

$$p_c(s_{i,\max}, s_{i,\min}) \leq s_{i,\min} \leq \lambda_i \leq s_{i,\max} \leq p_e(s_{i,\max}, s_{i,\min}), \tag{4}$$

where for all time $t_2 > t_1$

$$\begin{aligned} p_e(s_{i,\max}, s_{i,\min})\,|_{t_1} &\leq p_e(s_{i,\max}, s_{i,\min})\,|_{t_2} \\ p_c(s_{i,\max}, s_{i,\min})\,|_{t_1} &\geq p_c(s_{i,\max}, s_{i,\min})\,|_{t_2}, \end{aligned} \tag{5}$$

$p_e(s_{i,\max}, s_{i,\min}) \geq 1$, $p_c(s_{i,\max}, s_{i,\min}) \leq 1$ and $p_e(1,1) = p_c(1,1) = 1$. In general, $p_e \neq p_c$ and this asymmetry between tension and compression reflects on the asymmetry behaviour of stress-softening between tension and compression found in previous experiments [10]. An example of the functions p_e and p_c is

$$\begin{aligned} p_e(s_{i,\max}, s_{i,\min}) &= s_{i,\max} + k_e(1/s_{i,\min} - 1), \\ p_c(s_{i,\max}, s_{i,\min}) &= \frac{s_{i,\min}}{\sqrt{1 + k_c(s_{i\,\max} - 1)}}, \end{aligned} \tag{6}$$

where $k_e\,, k_c \geq 0$ are material constants. In this paper we will only discuss p_e and p_c given by Eq. (6).

We define our damage point a_i via the following:

$$a_i = \begin{cases} p_e(s_{i,\max}, s_{i,\min}) & \text{when } \lambda_i > 1, \\ p_c(s_{i,\max}, s_{i,\min}) & \text{when } \lambda_i < 1, \\ \dfrac{p_e(s_{i,\max}, s_{i,\min}) + p_c(s_{i,\max}, s_{i,\min})}{2} & \text{when } \lambda_i = 1. \end{cases} \tag{7}$$

In view of the properties of g, it is clear that $g(\lambda_i) \leq g(a_i)$. Physically, $g(a_i)$ can be considered as a measure of an amount of damage. The higher the value of $g(a_i)$, the bigger the damage caused by the deformation will be on the $\boldsymbol{e}_i$ principal-direction line element.

2.3 Shear-history parameters

There seem to be a lack of shearing experimental data to sufficiently analyse the effect of shearing on stress-softening materials; this prevent us from being able to accurately analyse the role of shear-history parameters in softening materials. However, previous isotropic models [4, 7] could predict experiments (where the shear values are zero) just using the principal stretches, and in [11] an experiment regarding the behaviour of a softening rubber material in simple shear is described. With this limited information, we consider the shear-history parameters

$$\begin{aligned} &b_{12} = b_{21} = v_{12,\max} + v_{12,\min}, \\ &b_{23} = b_{32} = v_{23,\max} + v_{23,\min}\,, \quad b_{13} = b_{31} = v_{13,\max} + v_{13,\min}, \end{aligned} \tag{8}$$

in our model, where

$$\begin{aligned} v_{ij,\max} = v_{ji,\max} &= \max_{0\le z\le t} \frac{\boldsymbol{e}_i \bullet \boldsymbol{U}^2(z)\boldsymbol{e}_j}{\sqrt{\boldsymbol{e}_i \bullet \boldsymbol{U}^2(z)\boldsymbol{e}_i}\sqrt{\boldsymbol{e}_j \bullet \boldsymbol{U}^2(z)\boldsymbol{e}_j}} \ge 0 \\ v_{ij,\min} = v_{ji,\min} &= \min_{0\le z\le t} \frac{\boldsymbol{e}_i \bullet \boldsymbol{U}^2(z)\boldsymbol{e}_j}{\sqrt{\boldsymbol{e}_i \bullet \boldsymbol{U}^2(z)\boldsymbol{e}_i}\sqrt{\boldsymbol{e}_j \bullet \boldsymbol{U}^2(z)\boldsymbol{e}_j}} \le 0 \quad (i \ne j : i,j = 1,2,3), \end{aligned} \tag{9}$$

taking note that, e.g., $b_{12} = b_{23} = b_{13} = 0$ in uniaxial deformations in a fixed direction. Here $v_{ij,\max}$ and $v_{ij,\min}$ are the maximum and minimum values of the cosine of the angle between the two principal-direction line elements throughout the history of the deformation. In this paper, we propose an energy function such that it can be easily modified to account for different types of shearing parameters if the need arises.

3 Constitutive equation

To describe anisotropic stress-softening the proposed energy function must be a function of $\boldsymbol{U}$ or λ_i and $\boldsymbol{e}_i$. The damage points and shear-history parameters are introduced into the energy function via the material parametric damage tensor $\boldsymbol{D}$ and shear-history tensor $\boldsymbol{S}$, respectively, viz.

$$\boldsymbol{D} = \sum_{i=1}^{3} g(a_i)\hat{\boldsymbol{e}}_i \otimes \hat{\boldsymbol{e}}_i \tag{10}$$

and

$$\boldsymbol{S} = \sum_{i,j=1}^{3} b_{ij}\hat{\boldsymbol{e}}_i \otimes \hat{\boldsymbol{e}}_j, \tag{11}$$

where we use the basis $\{\hat{\boldsymbol{e}}_i\} = \{\boldsymbol{e}_i\}$. Here we have defined $b_{11} = f_s(b_{12}, b_{13}), b_{22} = f_s(b_{21}, b_{23}), b_{33} = f_s(b_{31}, b_{32})$, with the property $f_s(0,0) = 0$. This condition is imposed since we choose, for simplicity, $\boldsymbol{S} = \boldsymbol{0}$ when $b_{12} = b_{23} = b_{13} = 0$. We note that both tensors $\boldsymbol{D}$ and $\boldsymbol{S}$ are symmetric and, in general, they are not constant during deformation. We postulate a parametric energy function W_f of the form

$$W_f = \tilde{W}(\boldsymbol{U}, \boldsymbol{D}, \boldsymbol{S}) = \bar{W}(\lambda_1, \lambda_2, \lambda_3, \boldsymbol{e}_1 \otimes \boldsymbol{e}_1, \boldsymbol{e}_2 \otimes \boldsymbol{e}_2, \boldsymbol{e}_3 \otimes \boldsymbol{e}_3, \boldsymbol{D}, \boldsymbol{S}). \tag{12}$$

For fixed $\boldsymbol{D}$ and $\boldsymbol{S}$ the energy function W_f represents an energy function of an anisotropic elastic material (see Sect. 3.2.1 for a clearer picture), where the anisotropic properties of the material are those which arise from the tensors $\boldsymbol{D}$ and $\boldsymbol{S}$. According to the work of Spencer [16], $\bar{W}$ is unchanged if the deformation field, the tensors $\boldsymbol{D}$ and $\boldsymbol{S}$ undergo a rotation which is described by a proper orthogonal tensor $\boldsymbol{Q}$. Thus

$$\begin{aligned} &\bar{W}(\lambda_1, \lambda_2, \lambda_3, \boldsymbol{e}_1 \otimes \boldsymbol{e}_1, \boldsymbol{e}_2 \otimes \boldsymbol{e}_2, \boldsymbol{e}_3 \otimes \boldsymbol{e}_3, \boldsymbol{D}, \boldsymbol{S}) \\ &\quad = \bar{W}\big(\lambda_1, \lambda_2, \lambda_3, \boldsymbol{Q}\boldsymbol{e}_1 \otimes \boldsymbol{Q}\boldsymbol{e}_1, \boldsymbol{Q}\boldsymbol{e}_2 \otimes \boldsymbol{Q}\boldsymbol{e}_2, \boldsymbol{Q}\boldsymbol{e}_3 \otimes \boldsymbol{Q}\boldsymbol{e}_3, \boldsymbol{Q}\boldsymbol{D}\boldsymbol{Q}^T, \boldsymbol{Q}\boldsymbol{S}\boldsymbol{Q}^T\big) \end{aligned} \tag{13}$$

The above equation holds for all proper orthogonal tensors $\boldsymbol{Q}$ and is a statement that $\bar{W}$ is an isotropic invariant of $\boldsymbol{U}, \boldsymbol{D}$ and $\boldsymbol{S}$. Hence $\bar{W}$ is a function of the $\lambda_1\, \lambda_2\, \lambda_3$ and the invariants of $\boldsymbol{e}_1 \otimes \boldsymbol{e}_1, \boldsymbol{e}_2 \otimes \boldsymbol{e}_2, \boldsymbol{e}_3 \otimes \boldsymbol{e}_3$, $\boldsymbol{D}$ and $\boldsymbol{S}$ [16].

We note that our model can be easily modified to include additional material parametric tensors of the same order or higher if it can be shown that these tensors can predict anisotropic stress-softening more accurately.

3.1 A class of energy functions

In this paper we focus on a class of W_f that depends only on the invariants [17]

$$\lambda_i, \boldsymbol{e}_i \bullet \boldsymbol{D}\boldsymbol{e}_i, \boldsymbol{e}_i \bullet \boldsymbol{S}\boldsymbol{e}_i \quad (i = 1,2,3), \tag{14}$$

i.e.,

$$W_f = W(\lambda_1, \lambda_2, \lambda_3, \boldsymbol{d}, \boldsymbol{s}), \tag{15}$$

where $\boldsymbol{d} = (d_1, d_2, d_3)^T = (\boldsymbol{e}_1 \bullet \boldsymbol{D}\boldsymbol{e}_1, \boldsymbol{e}_2 \bullet \boldsymbol{D}\boldsymbol{e}_2, \boldsymbol{e}_3 \bullet \boldsymbol{D}\boldsymbol{e}_3)^T$ and $\boldsymbol{s} = (s_1, s_2, s_3)^T = (\boldsymbol{e}_1 \bullet \boldsymbol{S}\boldsymbol{e}_1, \boldsymbol{e}_2 \bullet \boldsymbol{S}\boldsymbol{e}_2, \boldsymbol{e}_3 \bullet \boldsymbol{S}\boldsymbol{e}_3)^T$. Since the tensor $\boldsymbol{D}$ measures damage, we require, for fixed $\boldsymbol{e}_i$, W_f to decrease monotonically as d_i increases. To satisfy this property we impose the condition

$$\frac{\partial W_f}{\partial d_i} < 0\,. \tag{16}$$

We also impose the condition

$$W(1,1,1,\boldsymbol{d},\boldsymbol{s}) = 0, \tag{17}$$

so that $W_f = 0$ in the stress-free reference state.

This class also contains W with the properties:

(a) If $a_1 = \lambda_1, a_2 = \lambda_2$ and $a_3 = \lambda_3$ then

$$W(\lambda_1, \lambda_2, \lambda_3, \boldsymbol{d}, \boldsymbol{0}) = \hat{W}(\lambda_1, \lambda_2, \lambda_3) + \tilde{\Phi}(\boldsymbol{d}), \tag{18}$$

where the constant $\tilde{\Phi}(\boldsymbol{d})$ has the property $\tilde{\Phi}(\boldsymbol{0}) = 0$ and $\hat{W}(\lambda_1, \lambda_2, \lambda_3) = \hat{W}(\lambda_1, \lambda_3, \lambda_2) = \hat{W}(\lambda_3, \lambda_1, \lambda_2)$ is a scalar isotropic function.

(b) When $\boldsymbol{S} = 0$ the Biot stress is coaxial with $\boldsymbol{U}$.

These properties are consistent with some previous models [4–6] which show that, in deformations such as simple tension and biaxial deformations, where $\boldsymbol{S} = \boldsymbol{0}$, the material response on a *primary loading path* (defined below) can be described by an isotropic scalar function of $\boldsymbol{U}$ and the Biot stress for these deformations are coaxial with $\boldsymbol{U}$. Since $\hat{W}$ is similar to a strain-energy function of a perfectly elastic material, we can use standard forms of the perfectly elastic strain-energy function to represent the function $\hat{W}$. Here we only consider a class of isotropic scalar functions which can be represented by the Valanis–Landel [18] separable form, i.e.,

$$\hat{W}(\lambda_1, \lambda_2, \lambda_3) = r(\lambda_1) + r(\lambda_2) + r(\lambda_3), \tag{19}$$

where r has a specific form given by

$$r(\lambda_i) = \int_1^{\lambda_i} \frac{f(y)}{y}\, \mathrm{d}y\,, \quad i = 1,2,3, \tag{20}$$

where $f(1) = 0, f(y) > 0$ for $y > 1$ and $f(y) < 0$ for $y < 1$ [19]. It is clear that $r(1) = 0, r'(1) = 0$ (where a prime signifies differentiation with respect to the argument of the function in question), $0 = r(1) \leq r(y)$ and $r(y)$ increases (strictly) monotonically away from $y = 1$. The condition $f'(1) = 2E/3$, where E is the ground state Young's modulus for the virgin material, gives the appropriate ground-state conditions for an isotropic virgin material [19].

We define a stress–strain path as a primary loading path when the stress–strain constitutive equation can be characterised by the energy function given by Eq. (18).

3.2 Specific form

A special form of energy function is proposed in this section which simplifies the analysis of three-dimensional problems and also simplifies the calculation of material constants via experimental data (see Sect. 6). The special form is

$$W_f = \sum_{i=1}^{3} \hat{r}(\lambda_i, d_i) + C_c \hat{f}(\lambda_1, \lambda_2, \lambda_3, \boldsymbol{d}, \boldsymbol{s}), \tag{21}$$

where $C_c \geq 0$ is a material constant. The function $\hat{r}$ has the form

$$\hat{r}(\lambda_i, d_i) = \int_1^{\lambda_i} \eta(g(y), d_i) \frac{f(y)}{y} \, \mathrm{d}y \, ,$$

where the softening function η is introduced to soften the stress and hence has the property $0 < \eta(g(\lambda_i), d_i) \leq \eta(d_i, d_i) = 1$. The condition $\hat{f}(\lambda_1, \lambda_2, \lambda_3, \boldsymbol{d}, \boldsymbol{0}) = 0$ is imposed so that the properties (a) and (b) given in Sect. 3.1 are satisfied. To satisfy Eq. (16) we impose the requirements $\dfrac{\partial \eta}{\partial d_i} < 0$ and $\dfrac{\partial \hat{f}}{\partial d_i} < 0, \quad (i = 1, 2, 3)$.

3.2.1 Simple tension

On specialising to a simple tension deformation, where $\lambda_1 = \lambda$, $\lambda_2 = \lambda_3 = \dfrac{1}{\sqrt{\lambda}}$, we have $1 \leq \lambda \leq \lambda_m$. In view of Eq. (7), we have, $a_1 = \lambda_m$, $a_2 = a_3 = \dfrac{1}{\sqrt{\lambda_m}}$, $d_1 = g(\lambda_m), d_2 = d_3 = g\left(\dfrac{1}{\sqrt{\lambda_m}}\right)$ and $\boldsymbol{s} = \boldsymbol{0}$. The energy function becomes

$$W_f = \hat{r}(\lambda, g(\lambda_m)) + 2\hat{r}\left(\frac{1}{\sqrt{\lambda}}, g\left(\frac{1}{\sqrt{\lambda_m}}\right)\right). \tag{22}$$

and the non-zero principal Biot stress t takes the form

$$t = \frac{\eta(g(\lambda), g(\lambda_m)) f(\lambda) - \eta\left(g\left(\frac{1}{\sqrt{\lambda}}\right), g\left(\frac{1}{\sqrt{\lambda_m}}\right)\right) f\left(\frac{1}{\sqrt{\lambda}}\right)}{\lambda}. \tag{23}$$

To obtain Eq. (23) we require the relation for the Biot stress $\boldsymbol{T}^{(1)}$, i.e.,

$$\boldsymbol{T}^{(1)} = \frac{\partial W_f}{\partial \boldsymbol{U}} - p\boldsymbol{U}^{-1} \, , \tag{24}$$

where p is the Lagrange multiplier associated with the incompressibility constraint. Equation (23) also requires expressions for the components $\left(\dfrac{\partial W_f}{\partial \boldsymbol{U}}\right)_{ij}$ of $\dfrac{\partial W_f}{\partial \boldsymbol{U}}$ relative to the basis $\{\boldsymbol{e}_i\}$. These expressions are given below:

$$\left(\frac{\partial W_f}{\partial \boldsymbol{U}}\right)_{ii} = \frac{\partial W_f}{\partial \lambda_i}\,, \tag{25}$$

$$\left(\frac{\partial W_f}{\partial \boldsymbol{U}}\right)_{ij} = \frac{\dfrac{\partial W_f}{\partial \boldsymbol{e}_i}\bullet \boldsymbol{e}_j - \dfrac{\partial W_f}{\partial \boldsymbol{e}_j}\bullet \boldsymbol{e}_i}{2(\lambda_i - \lambda_j)}\,, \quad \lambda_i \neq \lambda_j\,,\ \ i \neq j. \tag{26}$$

It is assumed that W_f has sufficient regularity to ensure that, as λ_i approaches λ_j, Eq. (26) has a limit. The derivations of Eqs. (25) and (26) are given in the Appendix since the relations are rarely used in the literature. The stress–strain curve described by Eq. (23) is the elastic (nominal-strain) unloading path for $1 \le \lambda \le \lambda_m$ and W_f in Eq. (22) represents the area under this path from $\lambda = 1$ up to the strain $\lambda \le \lambda_m$. Different values of λ_m give different elastic unloading paths. Hence the stress–strain constitutive Eq. (23) represents infinitely many elastic unloading paths parameterised by λ_m. Different elastic unloading paths correspond to different elastic materials. When this is generalised to a three-dimensional deformation, the proposed energy function given by Eq. (12) characterises the softening material by a set containing infinite different elastic materials parameterised by the tensors $\boldsymbol{D}$ and $\boldsymbol{S}$, as exemplified by t and W_f in the simple tension specialisation. Note that, when $\lambda = \lambda_m$, we have, $\eta(g(\lambda_m), g(\lambda_m)) = \eta\left(g\left(\frac{1}{\sqrt{\lambda_m}}\right), g\left(\frac{1}{\sqrt{\lambda_m}}\right)\right) = 1$ and the nominal stress has the value

$$t = \frac{f(\lambda) - f\left(\dfrac{1}{\sqrt{\lambda}}\right)}{\lambda} \tag{27}$$

which lies on the primary loading path.

3.3 Dissipation

If we treat the parameter $\boldsymbol{D}$ as an internal variable which describes an anisotropic damage effect characterised by a softening of the material, we could then regard the parametric energy function W_f as a free-energy function. With this in mind we will show that the free-energy function satisfies the Clausius–Duhem inequality given by the relation

$$\mathrm{DIS} = \mathrm{tr}(\boldsymbol{T}^{(1)}\dot{\boldsymbol{U}}) - \dot{W}_f \ge 0\,, \tag{28}$$

where tr denotes the trace of a second-order tensor and the superposed dot represents, for example, the time derivative. From $\det(\boldsymbol{U}) = 1$ (where det denotes the determinant of a tensor) we have $\mathrm{tr}(\boldsymbol{U}^{-1}\dot{\boldsymbol{U}}) = 0$. Hence $\mathrm{tr}(\boldsymbol{T}^{(1)}\dot{\boldsymbol{U}}) = \mathrm{tr}((\boldsymbol{T}^{(1)} + p\boldsymbol{U}^{-1})\dot{\boldsymbol{U}})$. Note that

$$\dot{W}_f = \mathrm{tr}\left(\frac{\partial W_f}{\partial \boldsymbol{U}}\dot{\boldsymbol{U}}\right) + \sum_{i=1}^{3}\frac{\partial W_f}{\partial d_i}\dot{d}_i, \text{ where } \dot{d}_i = \dot{g}(a_i).$$

In view of the above and Eq. (28), since $\dot{\boldsymbol{U}}$ is arbitrary, we have the Biot stress given by Eq. (24). From Eqs. (24) and (28) we have

$$\mathrm{DIS} = -\sum_{i=1}^{3}\frac{\partial W_f}{\partial d_i}\dot{d}_i. \tag{29}$$

In view of Eq. (5) and the properties of g, it is clear that $\dot{d}_i \ge 0$. Equation (16) ensures that $\mathrm{DIS} \ge 0$ which is consistent with the Clausius–Duhem inequality that indicates energy dissipation.

4 Uniaxial deformation

4.1 Ground-state Young's moduli

In order to have a clearer picture of our model, we consider the following sequence of uniaxial deformations:

(i) The virgin material is loaded up to a maximal strain $\lambda_m \geq 1$ and unloaded.
(ii) After deformation (i) the non-virgin material is compressed down to a minimal strain $\lambda_c \leq 1$ and unloaded.

In this type of deformation $\boldsymbol{s} = \boldsymbol{0}$ and hence the Biot stress is coaxial with $\boldsymbol{U}$ and the principal Biot stress t_i (i=1,2,3) takes the simple form

$$t_i = \frac{\eta_i(\lambda_i, a_i) f(\lambda_i) - p}{\lambda_i}, \tag{30}$$

where for $i = 1, 2, 3$, $\eta_i(\lambda_i, a_i) = \eta(g(\lambda_i), g(a_i))$ and $d_i = g(a_i)$.

We only dicuss the case when $k_e = k_c = 0$ in Eq. (6). In deformation (i) we have $\lambda_1 = \lambda$, $\lambda_2 = \lambda_3 = \dfrac{1}{\sqrt{\lambda}}$ and $1 \leq \lambda \leq \lambda_m$ and during unloading

$$s_{1,\max} = \lambda_m \quad s_{1,\min} = s_{2,\max} = s_{3,\max} = 1\,, \quad s_{2,\min} = s_{3,\min} = \frac{1}{\sqrt{\lambda_m}}.$$

The tensile axial stress during unloading for deformation (i) (λ,$\lambda_m > 1$) is given by Eq. (30). On differentiating Eq. (30) with respect to λ and evaluating the derivative at $\lambda = 1^+$, we obtain the damaged (softened) ground-state "Young's modulus" E_t in the λ_1-direction for simple tension (not compression), viz.

$$E_t = \frac{2E}{3}\eta_1(1^+, \lambda_m) + \frac{E}{3}\eta_2\left(1^-, \frac{1}{\sqrt{\lambda_m}}\right). \tag{31}$$

In Sect. 4.2 we show that the material is transversely isotropic with respect to the stress-free configuration after deformation (i). With this in mind, we can easily show that during unloading in deformation (ii)

$$\lambda_1 = \lambda \leq 1, \quad \lambda_2 = \lambda_3 = \frac{1}{\sqrt{\lambda}}, \quad s_{1,\max} = \lambda_m, \quad s_{1,\min} = \lambda_c\,, 1 \geq \lambda \geq \lambda_c$$
$$s_{3,\max} = s_{2,\max} = \frac{1}{\sqrt{\lambda_c}}\,, \quad s_{3,\min} = s_{2,\min} = \frac{1}{\sqrt{\lambda_m}}\,.$$

The compressive axial stress is

$$t_1 = \frac{\eta_1(\lambda, \lambda_c) f(\lambda) - \eta_2\left(\frac{1}{\sqrt{\lambda}}, \frac{1}{\sqrt{\lambda_c}}\right) f\left(\frac{1}{\sqrt{\lambda}}\right)}{\lambda}. \tag{32}$$

The simple compression ground-state Young's modulus E_c in the λ_1-direction is

$$E_c = \frac{2E}{3}\eta_1(1^-, \lambda_c) + \frac{E}{3}\eta_2\left(1^+, \frac{1}{\sqrt{\lambda_c}}\right). \tag{33}$$

In general, the values of E_c and E_t are different. For the undamaged material $\lambda_m = \lambda_c = 1$ and we have $E_t = E_c = E$, as expected.

4.2 Transverse isotropy

In this section we show that our model produces a transversely isotropic non-virgin material in the stress-free state after a simple tension deformation as indicated by, e.g., by Horgan et al. [6]. Consider the deformation (i) given in Sect. 4.1. During unloading the damage tensor $\boldsymbol{D}$ takes the form

$$\boldsymbol{D} = \boldsymbol{D}_t = g(a_1)\hat{\boldsymbol{e}}_1 \otimes \hat{\boldsymbol{e}}_1 + g(a_2)\hat{\boldsymbol{e}}_2 \otimes \hat{\boldsymbol{e}}_2 + g(a_3)\hat{\boldsymbol{e}}_3 \otimes \hat{\boldsymbol{e}}_3, \tag{34}$$

where $\hat{\boldsymbol{e}}_i = \boldsymbol{e}_i$, $a_1 = p_e(\lambda_m, 1) = a_{\max}$ and $a_2 = a_3 = p_c\left(1, \frac{1}{\sqrt{\lambda_m}}\right) = a_{\min}$. The above equation can be written as

$$\boldsymbol{D}_t = (g(a_{\max}) - g(a_{\min}))\hat{\boldsymbol{e}}_1 \otimes \hat{\boldsymbol{e}}_1 + g(a_{\min})\boldsymbol{I}\,, \tag{35}$$

where we have used the identity tensor $\boldsymbol{I} = \hat{\boldsymbol{e}}_1 \otimes \hat{\boldsymbol{e}}_1 + \hat{\boldsymbol{e}}_2 \otimes \hat{\boldsymbol{e}}_2 + \hat{\boldsymbol{e}}_3 \otimes \hat{\boldsymbol{e}}_3$ to obtain Eq. (35). The shear-history tensor $\boldsymbol{S}$ takes the value $\boldsymbol{0}$ during unloading. The anisotropic fourth-order tensor ground-state elastic modulus can be represented by the second derivative of W_f with respect to $\boldsymbol{U}$ (or $\boldsymbol{C} = \boldsymbol{U}^2$) evaluated at $\boldsymbol{U} = \boldsymbol{I}$ [20]. In view of Eqs. (12) and (35), the second derivative of W_f evaluated at $\boldsymbol{U} = \boldsymbol{U}_t = \lambda \boldsymbol{e}_1 \otimes \boldsymbol{e}_1 + \frac{1}{\sqrt{\lambda}}\boldsymbol{e}_2 \otimes \boldsymbol{e}_2 + \frac{1}{\sqrt{\lambda}}\boldsymbol{e}_3 \otimes \boldsymbol{e}_3$ is

$$\frac{\partial^2 \tilde{W}}{\partial \boldsymbol{U}^2}(\boldsymbol{U}_t, \boldsymbol{D}_t, \boldsymbol{0}) = \frac{\partial^2 W_t}{\partial \boldsymbol{U}^2}(\boldsymbol{U}_t, \hat{\boldsymbol{e}}_1 \otimes \hat{\boldsymbol{e}}_1)\,, \tag{36}$$

where $\tilde{W}(\boldsymbol{U}, \boldsymbol{D}_t, \boldsymbol{0}) = W_t(\boldsymbol{U}, \hat{\boldsymbol{e}}_1 \otimes \hat{\boldsymbol{e}}_1)$ and we have treated λ_m as a material constant. The stress-free ground state is reached when $\lambda \to 1$ and we write $\boldsymbol{I}^+ = \lim_{\lambda \to 1} \boldsymbol{U}_t$. Hence, the second derivative of W_f at ground-state configuration takes the form

$$\frac{\partial^2 W_t}{\partial \boldsymbol{U}^2}(\boldsymbol{I}^+, \hat{\boldsymbol{e}}_1 \otimes \hat{\boldsymbol{e}}_1)\,. \tag{37}$$

Essentially, $\boldsymbol{I}^+ = \boldsymbol{I}$ and the fourth-order ground-state tensor modulus of a transversely isotropic material is represented by Eq. (37) [16]. This indicates that, in a uniaxial deformation, such as simple tension deformation, the proposed model produces a transversely isotropic material relative to the non-virgin stress-free unloaded state.

5 Application to simple homogeneous deformations

To further validate our anisotropic theory we study several types of simple homogeneous deformation. Some of our results are, qualitatively, compared with the experimental data of Pawelski [10]. For the purpose of illustration we consider

$$f(\lambda) = E\left(\frac{2}{3}\log(\lambda) + \frac{2}{3}(\mathrm{e}^{1-\lambda} + \lambda - 2)\right)$$

and use $E = \frac{3}{2}$ MPa for the virgin ground state Young's modulus. The damage function is assumed to have the form

$$g(x) = \begin{cases} x - 1 & \text{when } x \geq 1, \\ \frac{1}{x^2} - 1 & \text{when } x \leq 1. \end{cases} \tag{38}$$

In all the figures, the term "strain" means the (relevant) principal stretch.

5.1 Plane-strain compression in different directions and Pawelski's [10] experiment

Let (x_1, x_2, x_3) and (X_1, X_2, X_3) be the Cartesian components of $\boldsymbol{x}$ and $\boldsymbol{X}$, respectively. Initially, the virgin material is compressed in the X_2-direction down to a minimal strain λ_m and then unloaded. After this deformation we consider homogeneous plane-strain compressions in different directions where the angle

θ of direction is subtended from the X_1-axes in an anticlockwise direction. The axes of $\boldsymbol{X}$ are fixed in space.* *We note that this type of deformation may be cumbersome (or impossible) to simulate practically since it may involve cutting some part of the material so that a homogeneous plane-strain compression can be performed practically*. However, theoretical investigation of this type of deformation is useful for studying the anisotropic behaviour of a Mullins material. Initially the axes for the vectors $\boldsymbol{x}$ and $\boldsymbol{X}$ coincide. For a compression at an angle θ, the in-plane axes for the vector $\boldsymbol{x}$ rotate by the same angle and the compression load is applied parallel to the x_2-axes. Hence the deformation can be described by the equations

$$x_1 = \frac{1}{\lambda}(X_1 c + X_2 s), \quad x_2 = \lambda(-X_1 s + X_2 c), \quad x_3 = X_3\,, \tag{39}$$

where $c = \cos(\theta)$ and $s = \sin(\theta)$. We restrict ourselves to the intervals $0 \leq \theta \leq \dfrac{\pi}{2}$ and $1 \geq \lambda \geq \lambda_m$.

The principal direction components of $\boldsymbol{U}$ take the form

$$e_1 = \begin{bmatrix} c \\ s \\ 0 \end{bmatrix} \quad e_2 = \begin{bmatrix} -s \\ c \\ 0 \end{bmatrix} \quad e_3 = \begin{bmatrix} 0 \\ 0 \\ 1 \end{bmatrix} \tag{40}$$

and the principal stretches take the values

$$\lambda_1 = \frac{1}{\lambda}, \quad \lambda_2 = \lambda, \quad \lambda_3 = 1\,. \tag{41}$$

In this section we only consider $k_e = k_c = 0$. Virgin loading is applied by starting at time $t = 0$ and at $\theta = 0$ down to a minimal strain $\lambda = \lambda_m$ and is then unloaded until it is in a stress-free configuration. We let $t = t_1$ when this configuration is reached and denote this deformation by def(A). After deformation def(A) the non-virgin material is reloaded in a different or the same direction down to a minimal strain λ_m, taking note of statement* above.

Let

$$\hat{s}_{i,\max} = \max_{0 \leq z \leq t_1} \sqrt{\boldsymbol{e}_i \bullet \boldsymbol{U}^2(z)\boldsymbol{e}_i}, \quad \hat{s}_{i,\min} = \min_{0 \leq z \leq t_1} \sqrt{\boldsymbol{e}_i \bullet \boldsymbol{U}^2(z)\boldsymbol{e}_i}\,. \tag{42}$$

With a little algebra the optimised values can be written:

$$\hat{s}_{1,\max} = \begin{cases} \sqrt{\left(\dfrac{1}{\lambda_m^2} - \lambda_m^2\right)c^2 + \lambda_m^2}\,, & 1 \geq c > \dfrac{\lambda_m}{\sqrt{1+\lambda_m^2}} \\[2ex] 1\,, & 0 \leq c \leq \dfrac{\lambda_m}{\sqrt{1+\lambda_m^2}} \end{cases}, \tag{43}$$

$$\hat{s}_{1,\min} = \begin{cases} 1\,, & 1 \geq c \geq \sqrt{0{\cdot}5} \\ \sqrt{2c\sqrt{1-c^2}}\,, & \sqrt{0.5} > c \geq \dfrac{\lambda_m^2}{\sqrt{1+\lambda_m^2}} \\[2ex] \sqrt{\left(\dfrac{1}{\lambda_m^2} - \lambda_m^2\right)c^2 + \lambda_m^2}\,, & 0 \leq c < \dfrac{\lambda_m^2}{\sqrt{1+\lambda_m^2}} \end{cases}, \tag{44}$$

$$\hat{s}_{2,\max} = \begin{cases} \sqrt{\left(\frac{1}{\lambda_m^2} - \lambda_m^2\right) s^2 + \lambda_m^2}\,, & 1 \geq s > \frac{\lambda_m}{\sqrt{1+\lambda_m^2}}\,, \\ 1\,, & 0 \leq s \leq \frac{\lambda_m}{\sqrt{1+\lambda_m^2}} \end{cases} \tag{45}$$

$$\hat{s}_{2,\min} = \begin{cases} 1\,, & 1 \geq s \geq \sqrt{0.5} \\ \sqrt{2s\sqrt{1-s^2}}\,, & \sqrt{0.5} > s \geq \frac{\lambda_m^2}{\sqrt{1+\lambda_m^2}}\,, \\ \sqrt{\left(\frac{1}{\lambda_m^2} - \lambda_m^2\right) s^2 + \lambda_m^2}\,, & 0 \leq s < \frac{\lambda_m^2}{\sqrt{1+\lambda_m^2}} \end{cases} \tag{46}$$

$$\hat{s}_{3,\max} = \hat{s}_{3,\min} = 1. \tag{47}$$

The maximum and minimum values for the principal-direction line elements during reloading when $1 \geq \lambda \geq \lambda_m$ are

$$s_{i,\max} = \begin{cases} \hat{s}_{i,\max}\,, & 1 \leq \lambda_i \leq \hat{s}_{i,\max} \\ \lambda_i\,, & \hat{s}_{i,\max} < \lambda_i \leq \frac{1}{\lambda_m} \end{cases} \tag{48}$$

$$s_{i,\min} = \begin{cases} \hat{s}_{i,\min}\,, & 1 \geq \lambda_i \geq \hat{s}_{i,\min} \\ \lambda_i\,, & \hat{s}_{i,\min} > \lambda_i \geq \lambda_m \end{cases}. \tag{49}$$

In the case of re-loadings at $\theta = 0$ and $\theta = 90$ degrees it can be easily shown that $\boldsymbol{s} = \boldsymbol{0}$. However, $\boldsymbol{s} \neq 0$ for re-loadings not at 0 and 90 degrees; in this case, for simplicity of calculation, we only consider a material with the material constant $C_c = 0$. Results for $C_c \neq 0$ will be dealt with in the near future. Hence, for re-loading in any direction the Biot stress is coaxial with $\boldsymbol{U}$. The compressive principal Cauchy stress then takes the form

$$\sigma_2 = \sigma_v = f(\lambda) - f\left(\frac{1}{\lambda}\right) \tag{50}$$

for loading from a virgin state and

$$\sigma_2 = \sigma_n = \eta_2(\lambda, s_{2,\min}) f(\lambda) - \eta_1\left(\frac{1}{\lambda}, s_{1,\max}\right) f\left(\frac{1}{\lambda}\right) \tag{51}$$

for unloading. Its clear that

$$|\sigma_v| \geq |\sigma_n|$$

since $0 < \eta_i \leq 1$, $f(\lambda) \leq 0$ and $f\left(\frac{1}{\lambda}\right) \geq 0$. In Fig. 1 we depict the compressive stress-deformation for $\lambda_m = \frac{1}{2}$, virgin loading at an angle $\theta = 0$, unloading and reloadings after deformation def(A) at angles θ =0, 30, 45, 90 degrees.

It is clear from Fig. 1 that, as the angle θ increases, the compressive stress becomes less softened. In the case when the angle $\theta = 90$ degrees, the stress–strain curve behaves similarly to the virgin stress–strain curve, i.e., as if the material is not *softened*; this behaviour is close to that indicated empirically in Pawelski's experiment [10] and is described theoretically below. In the 90 degrees case we have

$$\hat{s}_{1,\max} = 1,\ \hat{s}_{1,\min} = \lambda_m,\ \hat{s}_{2,\max} = \frac{1}{\lambda_m},\ \hat{s}_{2,\min} = 1.$$

Hence

$$s_{2,\min} = \lambda\,,\quad s_{1,\max} = \frac{1}{\lambda}\,,\quad \sigma_2 = \eta_2(\lambda,\lambda)f(\lambda) - \eta_1\left(\frac{1}{\lambda},\frac{1}{\lambda}\right)f\left(\frac{1}{\lambda}\right) = f(\lambda) - f\left(\frac{1}{\lambda}\right) \tag{52}$$

since $\eta_2(\lambda,\lambda) = \eta_1\left(\frac{1}{\lambda},\frac{1}{\lambda}\right) = 1$. This stress is equal to σ_2 given in Eq. (50) for the virgin loading.

If after unloading the material from the 90 degree reloading, it is reloaded at 0 degree, we have

$$s_{1,\max} = \frac{1}{\lambda_m}\quad s_{2,\min} = \lambda_m\,,\quad s_{1,\min} = \lambda_m\,,\quad s_{2,\max} = \frac{1}{\lambda_m}\,. \tag{53}$$

The compressive stress is

$$\sigma_2 = \sigma_n = \eta_2(\lambda, s_{2,\min})f(\lambda) - \eta_1\left(\frac{1}{\lambda}, s_{1,\max}\right)f\left(\frac{1}{\lambda}\right), \tag{54}$$

which is the same as the stress given in Eq. (51). This behaviour is also indicated by Pawelski [10], i.e., the softening behaviour is not reduced, even after a perpendicular compression down to $\lambda = \lambda_m$.

5.2 Simple shear in different directions

In this section we investigate simple shear deformations where the principal directions of $\boldsymbol{U}$ change continuously during the deformation. Here, we only consider the case for a $C_c = 0$ material and damage points with $k_e = k_c = 0$. Hence the Biot stress is always coaxial with $\boldsymbol{U}$.

5.2.1 Virgin loading and reloading in the same direction

Here we let the axes of $\boldsymbol{x}$ and $\boldsymbol{X}$ to coincide and the deformation can be described by the equations

$$x_1 = X_1 + \gamma X_2,\quad x_2 = X_2,\quad x_3 = X_3, \tag{55}$$

where $0 \le \gamma \le \gamma_m$ and γ is commonly called *the amount of shear*. Let θ denote the orientation (in the anticlockwise sense relative to the X_1-axis) of the in-plane Lagrangean principal axes. The angle θ is restricted according to Ogden [21]:

$$\frac{\pi}{4} \le \theta < \frac{\pi}{2}\,. \tag{56}$$

The principal directions have the components

$$e_1 = \begin{bmatrix} c \\ s \\ 0 \end{bmatrix}\quad e_2 = \begin{bmatrix} -s \\ c \\ 0 \end{bmatrix}\quad e_3 = \begin{bmatrix} 0 \\ 0 \\ 1 \end{bmatrix}, \tag{57}$$

where $c = \cos(\theta)$ and $s = \sin(\theta)$. It can be easily shown that the principal stretches take the values

$$\lambda_1 = \frac{\gamma + \sqrt{\gamma^2+4}}{2} \ge 1,\quad \lambda_2 = \frac{1}{\lambda_1} = \frac{\sqrt{\gamma^2+4} - \gamma}{2} \le 1,\quad \lambda_3 = 1 \tag{58}$$

and

$$c = \frac{1}{\sqrt{1+\lambda_1^2}},\quad s = \frac{\lambda_1}{\sqrt{1+\lambda_1^2}},\quad \tan(2\theta) = -\frac{2}{\gamma},\quad \tan(\theta) = \lambda_1. \tag{59}$$

Consider the following sequence of deformations:

(i) the virgin material is subjected to a simple shear deformation up to $\gamma = \gamma_m$ and then unloaded;
(ii) The non-virgin material is reloaded in the same direction up to $\gamma = \gamma_m$.

For the deformation (ii) we have, for fixed c and s,

$$\begin{aligned} s_{1,\max} &= \max_{0\le\gamma\le\gamma_m} \sqrt{(\gamma s + c)^2 + s^2}, \quad s_{1,\min} = \min_{0\le\gamma\le\gamma_m} \sqrt{(\gamma s + c)^2 + s^2}, \\ s_{2,\max} &= \max_{0\le\gamma\le\gamma_m} \sqrt{(\gamma c - s)^2 + c^2}, \; s_{2,\min} = \min_{0\le\gamma\le\gamma_m} \sqrt{(\gamma c - s)^2 + c^2}, \\ s_{3,\max} &= s_{3,\min} = 1 \end{aligned} \tag{60}$$

Upon a little analysis we get

$$s_{1,\max} = \sqrt{(\gamma_m s + c)^2 + s^2}, \quad s_{1,\min} = 1\,, \quad 0 \le \gamma \le \gamma_m\,, \quad \gamma_m \ge 0$$

For $0 \le \gamma_m \le 2$

$$s_{2,\max} = 1\,, \quad 0 \le \gamma \le \gamma_m$$

and for $\gamma_m > 2$

$$s_{2,\max} = \begin{cases} \sqrt{(\gamma_m c - s)^2 + c^2}\,, & 0 \le \gamma \le \dfrac{\gamma_m^2 - 4}{2\gamma_m}\,, \\ 1\,, & \dfrac{\gamma_m^2 - 4}{2\gamma_m} < \gamma \le \gamma_m \end{cases}.$$

For $\gamma_m > 1$

$$s_{2,\min} = \begin{cases} c\,, & 0 \le \gamma < \dfrac{\gamma_m^2 - 1}{\gamma_m} \\ \sqrt{(\gamma_m c - s)^2 + c^2}\,, & \dfrac{\gamma_m^2 - 1}{\gamma_m} \le \gamma \le \gamma_m \end{cases}.$$

and for $0 \le \gamma_m \le 1$

$$s_{2,\min} = \sqrt{(\gamma_m c - s)^2 + c^2} \qquad 0 \le \gamma \le \gamma_m.$$

The shear components σ_{12} of the Cauchy stress for the deformations are:

$$\sigma_{12} = (f(\lambda_1) - f(\lambda_2))\hat{c}\hat{s} \tag{61}$$

for the virgin loading deformation (i) and

$$\sigma_{12} = [\eta_1(\lambda_1, s_{1,\max}) f(\lambda_1) - \eta_2(\lambda_2, s_{2,\min}) f(\lambda_2)]\hat{c}\hat{s} \tag{62}$$

for unloading in deformation (i) and reloading in deformation (ii). The terms $\hat{c}$ and $\hat{s}$ are given by

$$\hat{c} = \frac{1}{\sqrt{1+\lambda_2^2}}\,, \quad \hat{s} = \frac{\lambda_2}{\sqrt{1+\lambda_2^2}}\,.$$

Figure 2 depicts the loading and unloading curves for $\gamma_m = 2$ and $\gamma_m = 3$. It is clear from the figure that the stress-deformation curves behave as expected.

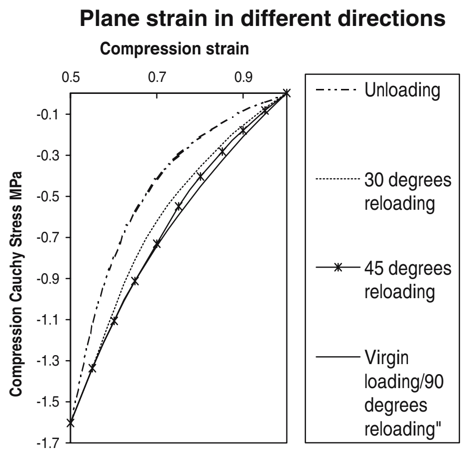

Fig. 1 Plane-strain compression in different directions

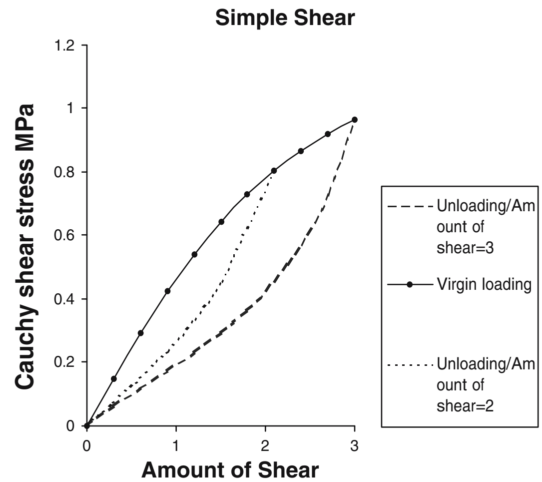

Fig. 2 Simple shear—loading and unloading

5.2.2 Reloading in the opposite direction

In this section, for simplicity we only consider $\gamma_m = 2$. Consider the following sequence of deformations:

(i) the virgin material is subjected to a simple shear deformation up to $\gamma = \gamma_m = 2$ and then unloaded.
(ii) The non-virgin material is reloaded in the opposite direction up to $\gamma = \gamma_m = 2$.

Here we have, for deformation (ii)

$$e_1 = \begin{bmatrix} -c \\ s \\ 0 \end{bmatrix} \quad e_2 = \begin{bmatrix} s \\ c \\ 0 \end{bmatrix} \quad e_3 = \begin{bmatrix} 0 \\ 0 \\ 1 \end{bmatrix},$$

where $c = \cos(\alpha)$, $s = \sin(\alpha)$ and
$\frac{\pi}{4} \le \alpha < \frac{\pi}{2}$.

Let t_1 be the time after deformation (i) is completed and

$$\hat{s}_{i,\max} = \max_{0 \le z \le t_1} \sqrt{\boldsymbol{e}_i \bullet \boldsymbol{U}^2(z)\boldsymbol{e}_i}$$

$$\hat{s}_{i,\min} = \min_{0 \le z \le t_1} \sqrt{\boldsymbol{e}_i \bullet \boldsymbol{U}^2(z)\boldsymbol{e}_i},$$

We then have

$$\hat{s}_{1,\max} = \sqrt{(2s-c)^2 + s^2}, \quad \hat{s}_{1,\min} = s, \quad \frac{\pi}{4} \le \alpha \le \tan^{-1}(1+\sqrt{2}),$$

$$\hat{s}_{2,\max} = \sqrt{(2c+s)^2 + c^2}, \quad \hat{s}_{2,\min} = 1, \quad \frac{\pi}{4} \le \alpha \le \tan^{-1}(1+\sqrt{2}).$$

The maximum and minimum values for the relevant principal-stretch line elements when $0 \le \gamma \le 2$ are

$$s_{1,\max} = \begin{cases} \hat{s}_{1,\max}, & 1 \le \lambda_1 \le \hat{s}_{1,\max} \\ \lambda_1, & \hat{s}_{1,\max} < \lambda_1 \le 1+\sqrt{2}, \end{cases}$$

$$s_{2,\min} = \begin{cases} \hat{s}_{2,\min}, & 1 \ge \lambda_2 \ge \hat{s}_{2,\min} \\ \lambda_2, & \hat{s}_{2,\min} > \lambda_2 \ge \sqrt{2}-1, \end{cases}$$

$$s_{3,\min} = s_{3,\max} = 1.$$

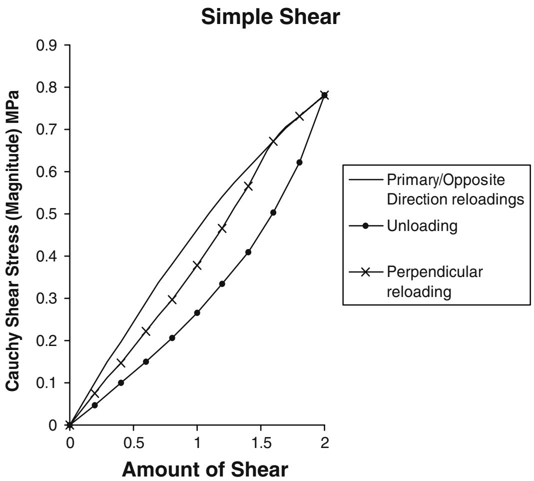

Fig. 3 Simple shear in different directions

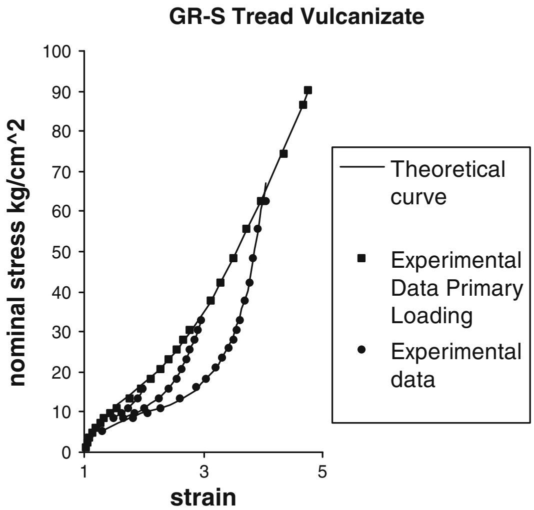

Fig. 4 Mullins and Tobin's [2] simple tension data

5.2.3 Reloading in a direction perpendicular to the initial plane of shear

In this section, for simplicity we only consider $\gamma_m = 2$. Consider the following sequence of deformations:

(i) the virgin material is subjected to a simple shear deformation up to $\gamma = \gamma_m = 2$ and then unloaded. Let t_1 be the time for this deformation.
(ii) The non-virgin material is reloaded in a direction perpendicular to the initial plane of shear up to $\gamma = \gamma_m = 2$.

Here we have, for deformation (ii)

$$e_1 = \begin{bmatrix} 0 \\ s \\ c \end{bmatrix} \quad e_2 = \begin{bmatrix} 0 \\ c \\ -s \end{bmatrix} \quad e_3 = \begin{bmatrix} 1 \\ 0 \\ 0 \end{bmatrix},$$

where c, s and α are defined in Sect. 5.2.2. We then have for t_1, $\hat{s}_{i,\max}$ and $\hat{s}_{i,\min}$ defined in Eq. (42)

$$\hat{s}_{1,\max} = \sqrt{4s^2 + 1}\,, \quad \hat{s}_{1,\min} = 1\,, \ \frac{\pi}{4} \le \alpha \le \tan^{-1}(1 + \sqrt{2}),$$

$$\hat{s}_{2,\max} = \sqrt{4c^2 + 1}\,, \quad \hat{s}_{2,\min} = 1\,, \ \frac{\pi}{4} \le \alpha \le \tan^{-1}(1 + \sqrt{2}).$$

The maximum and minimum values for the relevant principal-stretch line elements when $0 \le \gamma \le 2$ are

$$s_{1,\max} = \begin{cases} \hat{s}_{1,\max}\,, & 1 \le \lambda_1 \le \hat{s}_{1,\max} \\ \lambda_1\,, & \hat{s}_{1,\max} < \lambda_1 \le 1 + \sqrt{2} \end{cases},$$

$$s_{2,\min} = \begin{cases} \hat{s}_{2,\min}\,, & 1 \ge \lambda_2 \ge \hat{s}_{2,\min} \\ \lambda_2\,, & \hat{s}_{2,\min} > \lambda_2 \ge \sqrt{2} - 1 \end{cases}.$$

$$s_{3,\min} = s_{3,\max} = 1.$$

Figure 3 depicts results for various loadings given in this section. The theory closely predicts the experimental results of Muhr et al. [11]; they stated that "the softening is greatest for simple shear in the same direction, least for simple shear in the opposite direction and intermediate for shear at 90 degrees".

6 Comparison with experimental data

In this section we compare our theory with the experimental data of Mullins and Tobin [2], Mullins [22] and Gough [9] on simple tension and pure shear. For the sake of brevity we shall only use the isotropic scalar function proposed by Shariff [19], taking note that this form will only require a small number of linear equations to be solved when a curve-fitting method is used to obtain its parameter values [19]. According to [19] the component f of the energy function for the virgin material takes the form

$$f(\lambda) = E\sum_{i=0}^{n} \alpha_i \phi_i(\lambda)\,, \tag{63}$$

where α_i $(i = 1, 2, \ldots, n)$ are parameters with $\alpha_0 = 1$ and ϕ_is are sufficiently smooth functions such that $\phi_0(1) = 0, {\phi_0}'(1) = \frac{2}{3}, \phi_i(1) = {\phi_i}'(1) = 0, (i = 1, 2 \ldots, n)$. Specific forms for the functions ϕ_i, are

$$\begin{aligned} &\phi_0(\lambda) = \tfrac{2\log(\lambda)}{3}\,, \quad \phi_1(\lambda) = \mathrm{e}^{(1-\lambda)} + \lambda - 2\,, \; \phi_2(\lambda) = \mathrm{e}^{(\lambda-1)} - \lambda\,, \quad \phi_3(\lambda) = \tfrac{(\lambda-1)^3}{\lambda^{3.6}}, \\ &\phi_j = (\lambda - 1)^{j-1}, \quad j = 4, 5, \ldots, n. \end{aligned} \tag{64}$$

The function r takes the form

$$r(\lambda) = E\sum_{0}^{n} \alpha_i \Phi_i\,, \quad \Phi_i = \int_1^{\lambda} \frac{\phi_i(s)}{s}\,\mathrm{d}s.$$

The α_i values are obtained via the least-squares method similar to that described in [19]. The value $n = 3$ is sufficient to fit the virgin data.

For simplicity we use g given in Eq. (38) and η_i takes the form

$$\eta_i = \mathrm{e}^{(g(\lambda_i)-g(a_i))b(g(\lambda_i),g(a_i))}. \tag{65}$$

We consider only the case when $k_e = k_c = 0$. The function b in Eq. (65) is assumed to be of polynomial form, i.e.,

$$b(y, y_m) = \sum_{i=0}^{n1} b_i(y_m)y^i\,, \tag{66}$$

where we assume

$$b_i(y_m) = \sum_{j=0}^{n2} b_{i,j} y_m^j\,. \tag{67}$$

It is shown later that this form only requires a few terms to fit the data and the values of $b_{i,j}$ are easily obtained from a linear system of equations given in Eq. (67), where the values for b_i are obtained via a linear least-squares method based on the natural logarithm. For the simple tension data, the theoretical tensile principal stress σ_2 takes the form

$$\sigma_2 = \eta_2(\lambda, s_{2,\max})f(\lambda) - \eta_3\left(\frac{1}{\sqrt{\lambda}}, s_{3,\min}\right) f\left(\frac{1}{\sqrt{\lambda}}\right), \tag{68}$$

where $1 \le \lambda \le s_{2,\max}$. Since $s_{3,\min} = s_{1,\min} = \dfrac{1}{\sqrt{s_{2,\max}}}$ and, in view of Eqs. (65–67), we have

$$\eta_2(\lambda, s_{2,\max}) = \eta_3\left(\frac{1}{\sqrt{\lambda}}, s_{3,\min}\right)\,. \tag{69}$$

Hence

$$\sigma_2 = \eta_2(\lambda, s_{2,\max})\left(f(\lambda) - f\left(\frac{1}{\sqrt{\lambda}}\right)\right)\,. \tag{70}$$

For the least-squares method we minimise the expression

$$E_r = \sum_j \left(\log\left(\eta_2(x_j, s_{2,\max}) \left(f(x_j) - f\left(\frac{1}{\sqrt{x_j}} \right) \right) \right) - \log(x_j z_j) \right)^2, \tag{71}$$

where x_j and z_j are the experimental strain and nominal stress values, respectively. The above minimising statement is equivalent to minimising

$$E_d = \sum_j \left(\sum_{i=0}^{n_1} b_i(s_{2,\max})(x_j - s_{2,\max}) x_j^i - d_j \right)^2, \tag{72}$$

where $d_j = \log\left(\dfrac{x_j z_j}{f(x_j) - f\left(\frac{1}{\sqrt{x_j}} \right)} \right)$, which is suitable for the linear least-squares method to obtain the b_i values. The $b_{i,j}$ coefficients are then obtained via a system of linear equations using Equation (67). For Mullins and Tobin's [2] and Mullins's [22] data we use the values $n_1 = 2$ and $n_2 = 2$ for the functions b and b_i, respectively, $s_{2,\max} = 2{\cdot}04, 3{\cdot}06, 4$ for Mullins's [22] data and $s_{2,\max} = 2, 3, 4{\cdot}02$ for the Mullins and Tobin [2] data.

The parameter values for the isotropic scalar function in Gough's [9] pure shear data are obtained in a similar fashion to the simple tension data. For the isotropic scalar function in pure shear we only need $n = 3$ to fit the components of the Cauchy principal stress

$$\sigma_1 = f(\lambda) - f\left(\frac{1}{\lambda} \right), \quad \sigma_2 = -f\left(\frac{1}{\lambda} \right) \tag{73}$$

to the data, where $1 \leq \lambda \leq s_{1,\max} = 2$. For the non-virgin material the reloading data of the stresses $\sigma_1 - \sigma_2$ and σ_2 are used to obtain the b_i values. We only need to use the value $n_1 = 2$ to fit the data. In order to obtain a unique solution for the parameters $b_{i,j}$ the value $n_2 = 1$ is used. In this case

$$\sigma_1 - \sigma_2 = \eta_1(\lambda, 2) f(\lambda), \quad \sigma_2 = -\eta_3\left(\frac{1}{\lambda}, \frac{1}{2} \right) f\left(\frac{1}{\lambda} \right), \tag{74}$$

taking into account that $\lambda_2 = 1$ and $f(1) = 0$.

The curve-fitted values of the parameters are: Mullins and Tobin [2]:

$$E = 37{\cdot}063\,\text{kg/cm}^2, \quad \alpha_1 = -2{\cdot}900, \quad \alpha_2 = -0{\cdot}074, \quad \alpha_3 = 7{\cdot}187$$
$$b_{0,0} = 73{\cdot}982, \quad b_{0,1} = -44{\cdot}103, \quad b_{0,2} = 6{\cdot}395$$
$$b_{1,0} = -98{\cdot}162, \quad b_{1,1} = 58{\cdot}243, \quad b_{1,2} = -8{\cdot}418$$
$$b_{2,0} = 33{\cdot}288, \quad b_{2,1} = -19{\cdot}566, \quad b_{2,2} = 2{\cdot}813$$

Mullins [22]:

$$E = 55.826\,\text{kg/cm}^2, \quad \alpha_1 = -3{\cdot}958, \quad \alpha_2 = -0{\cdot}161, \quad \alpha_3 = 9{\cdot}072$$
$$b_{0,0} = -10{\cdot}378, \quad b_{0,1} = 2{\cdot}308, \quad b_{0,2} = 0{\cdot}085$$

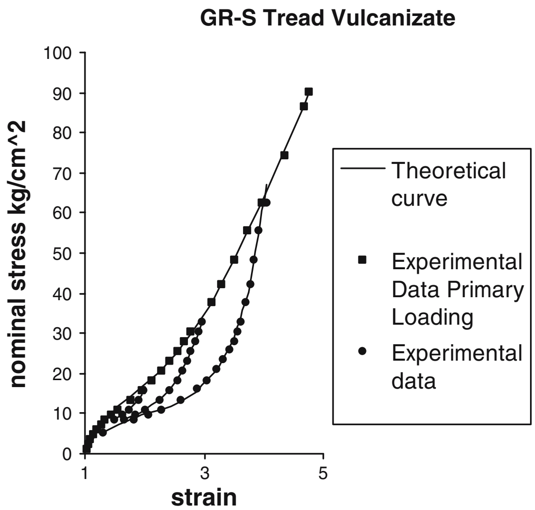

Fig. 5 Mullins [22] simple tension data

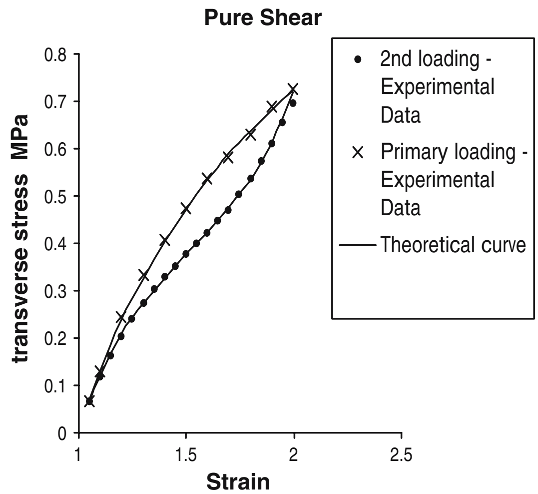

Fig. 6 Fitted curves for Gough's [9] pure shear data

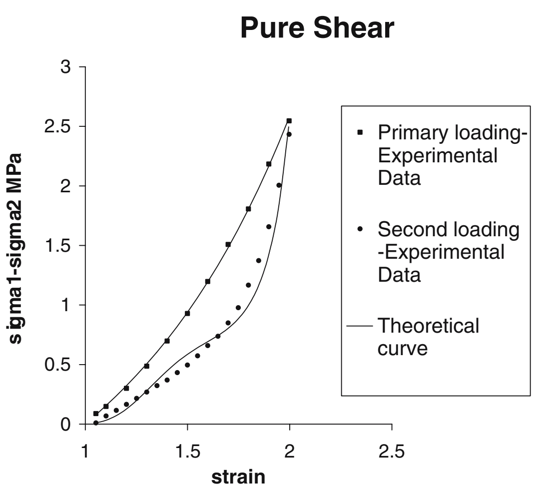

Fig. 7 Fitted curves for Gough's [9] pure shear data

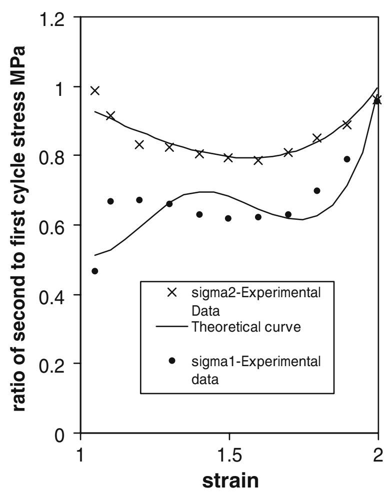

Fig. 8 Predicting Gough's [9] data

$$b_{1,0} = 16{\cdot}122, \quad b_{1,1} = -5{\cdot}447, \quad b_{1,2} = 0{\cdot}3454$$
$$b_{2,0} = -4{\cdot}8153, \quad b_{2,1} = 1{\cdot}909, \quad b_{2,2} = -0{\cdot}1696$$

Gough [9]:

$$E = 2{\cdot}270\,\text{MPa}, \quad \alpha_1 = 0{\cdot}225, \quad \alpha_2 = 0{\cdot}860, \quad \alpha_3 = -0{\cdot}074$$
$$b_{0,0} = 49{\cdot}066, \quad b_{0,1} = -12{\cdot}268$$
$$b_{1,0} = -68{\cdot}933, \quad b_{1,1} = 17{\cdot}252$$
$$b_{2,0} = 24{\cdot}935, \quad b_{2,1} = -6{\cdot}233$$

In Figs. 4–7 we observe that the theoretical curves fit very well with the experimental data. Using the parameter values given above we *predict* (not curve-fitted) the deformations shown in Figs. 8 and 9. Our

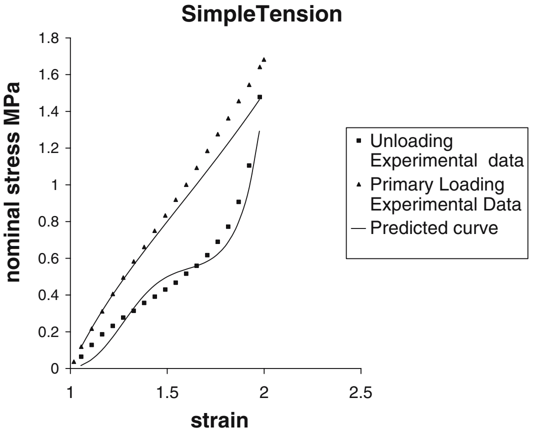

Fig. 9 Predicting Gough's [9] simple tension data

theory predicts the actual stress-deformation data reasonably well. We note that the data in Fig. 8 cannot be predicted using an isotropic constitutive equation of the form

$$\boldsymbol{T} = \eta_s(\lambda_1, \lambda_2, \alpha_m)\frac{\partial \hat{W}}{\partial \boldsymbol{U}}(\lambda_1(\boldsymbol{U}), \lambda_2(\boldsymbol{U}), \lambda_3(\boldsymbol{U})) - p\boldsymbol{U}^{-1}, \tag{75}$$

where α_m is a measure of an amount of damage and $0 < \eta_s \leq 1$.

7 Concluding remarks

Most of the constitutive models in the current literature describing the Mullins effect are based on isotropic stress-softening. However, stress-softening, in general, is an inherently anisotropic phenomenon. In this paper we describe this strain-induced anisotropic behaviour via a parametric energy function which depends explicitly on the principal stretches and the principal directions. The material parameters in the energy function are second-order symmetric tensors $\boldsymbol{D}$ and $\boldsymbol{S}$, which measures the amount of damage caused by deformation and capture the effect of shear-history on stress-softening, respectively. We introduce the terms damage function and damage point here to facilitate our analysis of the proposed constitutive equation. We only discuss a class of energy functions which is a subset of a wider class of energy functions proposed in Sect. 3 and this discussion may provide insight into the construction of a more general and wider class of functions.

Since our approach is new and quite different from that reported elsewhere on stress-softening rubber mechanics, to further validate our anisotropic theory, we extensively discuss our results for various types of homogenous deformations. It is found that our theory compares fairly well with several anisotropic experimental results, and we have shown that predictions are consistent with expected behaviour. We have also shown that the proposed model produces a transversely isotropic material with respect to the stress-free configuration after unloading from a simple tension deformation. To the best of our knowledge, we believe that no previous models have managed to achieve the above-mentioned results.

So far we have shown that our theory predicts fairly well by just using the first (non-shear) term of the parametric energy function given by Eq. (21). The second (shear) term in Eq. (21) is not used at all in the predictions. However, in the near future we need to analyse the role of the second term in Mullins's induced anisotropy and this requires appropriate experimental data for $\boldsymbol{S} \neq \boldsymbol{0}$.

Appendix. Components of $\dfrac{\partial W_f}{\partial \boldsymbol{U}}$ relative to the basis $\{\boldsymbol{e}_i\}$

Let $\boldsymbol{U}=\sum_{i=1}^{3}\lambda_i \boldsymbol{e}_i\otimes\boldsymbol{e}_i$, where λ_i are the principal stretches. Then

$$(\mathrm{d}\boldsymbol{U})_{ij}=\mathrm{d}\lambda_i\delta_{ij}+(\lambda_j-\lambda_i)\boldsymbol{e}_i\bullet\mathrm{d}\boldsymbol{e}_j \tag{76}$$

are the differential components of $\mathrm{d}\boldsymbol{U}$ relative to the orthonormal basis $\boldsymbol{e}_i$ (see, e.g., [21]). Let

$$W_f=\tilde{W}(\boldsymbol{U},\boldsymbol{D},\boldsymbol{S})=\bar{W}(\lambda_1,\lambda_2,\lambda_3,\boldsymbol{e}_1\otimes\boldsymbol{e}_1,\boldsymbol{e}_2\otimes\boldsymbol{e}_2,\boldsymbol{e}_3\otimes\boldsymbol{e}_3,\boldsymbol{D},\boldsymbol{S})\,. \tag{77}$$

Then

$$\mathrm{d}W_f=\mathrm{tr}\left(\frac{\partial W_f}{\partial\boldsymbol{U}}\mathrm{d}\boldsymbol{U}\right)=\sum_{i,j=1}^{3}\left(\frac{\partial W_f}{\partial\boldsymbol{U}}\right)_{ij}(\mathrm{d}\boldsymbol{U})_{ij}=\sum_{i=1}^{3}\left(\frac{\partial W_f}{\partial\lambda_i}\mathrm{d}\lambda_i+\frac{\partial W_f}{\partial\boldsymbol{e}_i}\bullet\mathrm{d}\boldsymbol{e}_i\right), \tag{78}$$

where $\left(\dfrac{\partial W_f}{\partial\boldsymbol{U}}\right)_{ij}$ are the components of $\dfrac{\partial W_f}{\partial\boldsymbol{U}}$ relative to the basis $\{\boldsymbol{e}_i\}$. In view of Equations (76) and (78), since $\mathrm{d}\lambda_i$ is arbitrary, we have

$$\left(\frac{\partial W_f}{\partial\boldsymbol{U}}\right)_{ii}=\frac{\partial W_f}{\partial\lambda_i},\quad i\quad\text{not summed} \tag{79}$$

In order to evaluate the shear components

$$\left(\frac{\partial W_f}{\partial\boldsymbol{U}}\right)_{ij},\quad i\neq j \tag{80}$$

we take note that

$$\boldsymbol{e}_i\bullet\boldsymbol{e}_j=\delta_{ij} \tag{81}$$

and

$$\mathrm{d}\boldsymbol{e}_i\bullet\boldsymbol{e}_j+\boldsymbol{e}_i\bullet\mathrm{d}\boldsymbol{e}_j=0. \tag{82}$$

For $i=j$ we have $\mathrm{d}\boldsymbol{e}_i\bullet\boldsymbol{e}_i=0$ and we can deduce, via orthogonal subspaces, that

$$\mathrm{d}\boldsymbol{e}_1=\mathrm{d}a_{12}\boldsymbol{e}_2+\mathrm{d}a_{13}\boldsymbol{e}_3,\quad \mathrm{d}\boldsymbol{e}_2=\mathrm{d}a_{21}\boldsymbol{e}_1+\mathrm{d}a_{23}\boldsymbol{e}_3,\quad \mathrm{d}\boldsymbol{e}_3=\mathrm{d}a_{31}\boldsymbol{e}_1+\mathrm{d}a_{32}\boldsymbol{e}_2 \tag{83}$$

where $\mathrm{d}a_{ij}$'s are arbitrary but not fully independent, as shown below. From Eqs. (82) and (83) for $i\neq j$ we can deduce that

$$\mathrm{d}a_{ij}=-\mathrm{d}a_{ji} \tag{84}$$

We are now in a position to derive, for example, the expression for the term $\left(\dfrac{\partial W_f}{\partial\boldsymbol{U}}\right)_{12}=\left(\dfrac{\partial W_f}{\partial\boldsymbol{U}}\right)_{21}$, taking note that $\dfrac{\partial W_f}{\partial\boldsymbol{U}}$ is symmetric. From Eq. (78) we see that

$$\ldots\left(\frac{\partial W_f}{\partial\boldsymbol{U}}\right)_{12}(\mathrm{d}\boldsymbol{U})_{12}+\left(\frac{\partial W_f}{\partial\boldsymbol{U}}\right)_{21}(\mathrm{d}\boldsymbol{U})_{21}+\cdots=\cdots\frac{\partial W_f}{\partial\boldsymbol{e}_1}\bullet\mathrm{d}\boldsymbol{e}_1+\frac{\partial W_f}{\partial\boldsymbol{e}_2}\bullet\mathrm{d}\boldsymbol{e}_2\ldots \tag{85}$$

Substituting Eqs. (76) and (83) in Eq. (85), taking note of Equation (84) and the fact that $\mathrm{d}a_{12}$ is arbitrary, we have

$$\left(\frac{\partial W_f}{\partial\boldsymbol{U}}\right)_{12}=\frac{\dfrac{\partial W_f}{\partial\boldsymbol{e}_1}\bullet\boldsymbol{e}_2-\dfrac{\partial W_f}{\partial\boldsymbol{e}_2}\bullet\boldsymbol{e}_1}{2(\lambda_1-\lambda_2)}\,. \tag{86}$$

Similarly we can easily show that

$$\left(\frac{\partial W_f}{\partial\boldsymbol{U}}\right)_{ij}=\frac{\dfrac{\partial W_f}{\partial\boldsymbol{e}_i}\bullet\boldsymbol{e}_j-\dfrac{\partial W_f}{\partial\boldsymbol{e}_j}\bullet\boldsymbol{e}_i}{2(\lambda_i-\lambda_j)}\,. \tag{87}$$

References

1. Mullins L (1947) Effect of stretching on the properties of rubber. J Rubber Res 16:275–289
2. Mullins L, Tobin NR (1957) Theoretical model for the elastic behaviour of filler-reinforced vulcanized rubbers. Rubber Chem Technol 30:551–571
3. Govindjee S, Simo JC (1991) A micro-mechanically based continuum damage model for carbon black-filled rubbers incorporating the Mullin's effect. J Mech Phys Solids 39:87–112
4. Ogden RW, Roxburgh DG (1999) A pseudo-elastic model for the Mullins effect in filled rubber. Proc R Soc London A 455:2861–2877
5. Beatty MF, Krishnaswamy S (2000) A theory of stress-softening in incompressible isotropic materials. J Mech Phys Solids 48:1931–1965
6. Horgan CO, Ogden RW, Saccomandi G (2004) A theory of stress softening of elastomers based on finite chain extensibility. Proc R Soc London A 460:1737–1754
7. Qi HJ, Boyce MC (2004) Contitutive model for stretched-induced softening of the stress-stretch behavior of elastomeric materials. J Mech Phys Solids 52:2187–2205
8. James AG, Green A (1975) Strain energy functions of rubber. II. Characterisation of filled vulcanizates. J Appl Polym Sci 19:2033–2058
9. Gough J (2005) Stress-strain behaviour of rubber. PhD Thesis Queen Mary and Westfield College, University of London
10. Pawelski H (2001) Softening behaviour of elastomeric media after loading in changing directions. In: Besdo D, Schuster RH, Ihlemann J (eds) Constitutive models for rubber II. A.A. Balkema Lisse, The Netherlands, pp 27–36
11. Muhr AH, Gough J, Gregory IH (1999) Experimental determination of model for liquid silicone rubber. In: Muhr A, Dorfmann A (eds) Constitutive models for rubber. A.A. Balkema, Rotterdam, pp 181–187
12. Shariff MHBM (2005) Multiaxial anisotropic stress-softening constitutive equation. Kauchuk I Rezina 2:16–19
13. Shariff MHBM, Noor MA (2004) Anisotropic stress-softening model for damaged material. In: Proceedings of the seventh international conference on computational structures technology. Lisbon
14. Miehe C (1995) Discontinuous and continuous damage evolution in Ogden-type large strain elastic materials. Euro Jl Mech A 14:697–720
15. Laiarinandrasana L, Layouni K, Piques R (2001) Mullins effect on rubber materials: Damage model driving parameters, In: Besdo D, Schuster RH, and Ihlemann J (eds) Constitutive models for rubber II. A.A. Balkema Publishers Lisse (The Netherlands) pp 149–160
16. Spencer AJM (1984) Constitutive theory of strongly anisotropic solids. In: Spencer AJM (ed) Constitutive theory of the mechanics of fiber reinforced composites (chapter IX), CISM Courses and Lectures No. 282. Springer, Wien, pp 1–32
17. Spencer AJM (1971) Theory of invariants. In: Eringen AC (ed) Continuum physics I (Part III). Academic Press, New York, pp 239–353
18. Valanis KC, Landel RF (1967) The strain-energy function of hyperelastic material in terms of the extension ratios. J Appl Phys 38:2997–3002
19. Shariff MHBM (2000) Strain energy function for filled and unfilled rubberlike material. Rubber Chem Technol 73:1–21
20. Shariff MHBM, Parker DF (2000) An extension of Key's principle to nonlinear elasticity. J Engng Math 37:171–190
21. Ogden RW (1984) Non-linear deformations. John Wiley, New York
22. Mullins L (1969) Softening of rubber by deformation. Rubber Chem Technol 42:339–362